Residual hole concentration in recombination centres after bleaching

N. Pawlak[1], A. Timar-Gabor[2, 3], A. Chruścińska[1*]

[1] Institute of Physics, Faculty of Physics, Astronomy and Informatics, Nicolaus Copernicus University, Torun, Poland

[2] Faculty of Environmental Science and Engineering, Babeş-Bolyai University, Cluj-Napoca, Romania

[3] Interdisciplinary Research Institute on Bio-Nano-Sciences, Babeş-Bolyai University, Cluj-Napoca, Romania

Abstract

Trapped charge dating method using electron spin resonance (ESR) of quartz is progressively used for sediment dating. As in the case of luminescence dating methods, the ESR signals can be used for accurate age estimation of a sediment layer only when these signals are zeroed by sunlight exposure before the layer creation or when one knows their ESR residual level (in other words the part of the signal that is not bleached). It is well known that the ESR signal related the Al-hole centres in quartz used for sediment dating has a significant residual signal. From the point of view of luminescence models, as a hole trap, the Al-hole centre is considered a recombination centre in quartz. Recently, it was demonstrated experimentally that the ESR signal of Al-hole centre is dependent on the total dose absorbed by the quartz sample in the past. The same effect was confirmed by simulations of the charge transport processes for a model including two recombination centres. Here, the dependence of residual hole concentration in the recombination centres on the total dose absorbed by a sample in the past is studied in detail by computer simulations for a wide range of model parameters. The impact that the various relations of centre parameters have on the dependence of the residual as function of dose is investigated and the implications for the dating practice are discussed.

Keywords: bleaching, recombination centres, residual, quartz, Al-h ESR signal

1. Introduction

Trapped charge dating methods such as luminescence and electron spin resonance are increasingly used for sediment dating. The physical phenomena that these methods rely upon are based on the presence of trapping states in the crystalline structure of the minerals used. The concentration of electrons and/or holes held in these metastable states increases with continuous excitation of the charge by the natural background radiation and can be used to estimate the time elapsed since the traps were emptied, based on the assumption that the dose rate remained constant during time.

The key event in sediment dating is the formation of a sediment layer, i.e. the deposition of mineral grains after they have been transported by wind or water, and then covered with another layer. If any of the trapped charge methods are to be used for dating a sediment layer, the traps must be empty at the time of its formation, or the residual level must be known. The main natural factor responsible for trap emptying before grain deposition in the case of sediments is sunlight exposure, so only the traps which are sensitive to sunlight bleaching can be used for dating.

Two phenomena are exploited to measure the concentration of trapped charge when dating sediments: optically stimulated luminescence (OSL) and electron spin resonance (ESR). According to the current understanding of the OSL processes in the minerals commonly used for dating (quartz or potassium feldspars), OSL dating relies on the quantification of the concentration of trapped electrons. (Bailey and Arnold, 2006; Preusser et al., 2009; Peng and Pagonis, 2016; Friedrich et. al., 2016). On the other hand, in the case of electron spin resonance applied on quartz both electron (such as Ti centres) as well as hole traps (Al-hole centres) are used in the so-called Multiple Centre (MC) approach (Toyoda, et al., 2000; Duval and Guilarte, 2015). These hole traps play the role of recombination centres in luminescence models of minerals. However, from both luminescence and ESR measurements it is known that the recombination centres are not completely emptied even after extremely long time bleaching by light. When the sample is heated after the prolonged bleaching, the so-called residual thermoluminescence was reported by many (Aitken, 1998; Singhivi

et al., 1982; Smith and Rhodes, 1994; Spooner, 1994; Przegiętka et al., 2005; Chruścińska and Przegiętka, 2005). Similar effects have been found in ESR measurements on hole centres (Walther and Zilles, 1994; Toyoda and Falguéres, 2003; Duval et al., 2017; Bartz et al., 2020). When the Al-hole centre is used for dating it is common practice to quantify the residual concentration of holes, in other words measuring the intensity of residual ESR signal after bleaching and subtracting it from the measured ESR for accurate equivalent dose determination (Voinchet et al., 2003). There are two approaches to estimate the residual ESR signal. The first is to measure it after an exposure of many days to the sunlight simulator and express it as the percent of natural ESR signal measured without bleaching. The reported values vary between 40 % and 80 % (Walther and Zilles, 1994; Voinchet et al., 2003; Rink et al., 2007; Tsukamoto et al., 2017). Another way of residual ESR level estimation is the measurement of a modern analogue or the reconstruction of the natural dose response curves (i.e. the plot of intensity of the natural ESR signal versus the expected natural dose) using an extended sediment layer sequence for which an independent age control is available. The approximation of the residual signal is the intercept of the natural dose response curve (Tsukamoto et al., 2018). However, these methods assume that the ESR residual level was the same for all samples in the stratigraphic sequence and can be practically carried out only under fortunate circumstances when age information is already available.

A recent study has shown that the residual level of the Al-hole ESR centre in quartz depends on the total absorbed dose (Timar-Gabor et al., 2020). This effect is in line with the simulation results performed for the kinetic model of charge transport processes involving two recombination centres and several types of traps which are populated and emptied with the participation of the conduction band. The key to this phenomenon is the presence of deep traps that are thermally stable and are not emptied by light, the so-called disconnected traps. The occupation of these traps by electrons after the bleaching dictates that the recombination centres are filled with an identical number of holes. Their number is shared between the different recombination centres adequately to the probability of electron recombination in the centres. For equal concentrations of the recombination

centres, the residual level of holes is lower for the centre with the bigger recombination coefficient. The residual level of hole concentration in recombination centres after bleaching, i.e. also the residual ESR signal corresponding to this centre, increases with the total absorbed dose until doses that cause the saturation of the electron population in the disconnected traps. As such, the residual signal depends on the concentrations of the deep disconnected traps and recombination centres as well as on their parameters.

Detailed results of the simulation of the processes leading to residual hole concentration after optical bleaching are presented here for wide ranges of recombination centre parameters. The impact of the mutual relation of the parameters of individual recombination centres on the residual level of holes and the dependence of the residual level on dose is investigated. It is shown that for some ranges of the parameters the function describing the changes of residual hole concentration level with dose does not simply increase up to the highest value at doses for which the disconnected traps are most populated by electrons, but it rises and then decreases again. This, on the one hand makes the level of the residual hole concentration hard to predict and on the second hand, can provide some insights into the relation between the parameters of recombination centres in the field of research on the properties of luminescent materials. It should be mentioned that the processes presented below, although investigated in close relation to the application of ESR signal of the aluminum hole centre in quartz for dating, generally apply to the occupation of recombination centres in insulating crystals in a metastable state. The effects observed in the simulations may explain the changes in luminescence effectiveness in phosphors after prolonged irradiation and exposure to light. The presence of deep disconnected traps can lead to surprising effects.

2. **Methods**

The simulations were performed by means of MATLAB differential equation solver ode15s, which is the appropriate tool for stiff equations. The charge transfer in the crystal was simulated for 1) the process of excitation - the filling of the traps

105 2) the bleaching process.

106 The simulations were carried out for a kinetic model that includes four kinds of traps and two
107 recombination centres (Fig. 1). Traps of the first kind are shallower than the others, are optically
108 emptied during bleaching and are not thermally stable during irradiation. Traps of two other kinds
109 are optically emptied during the bleaching and are thermally stable during irradiation and bleaching.
110 The last kind of traps are deep and are neither optically nor thermally emptied in the simulated
111 processes. They will hereinafter be referred to as disconnected traps.

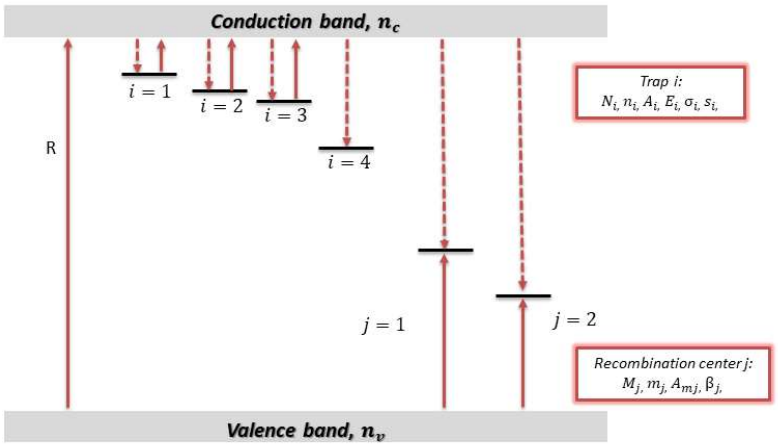

Fig. 1. Energy levels and transitions taken into account in the model used in the simulations.

112

113 The kinetic equations solved at both steps of simulations have the following form:

114 $$\frac{dn_i}{dt} = -n_i\sigma_i f - s_i \exp\left(\frac{-E_i}{kT}\right) n_i + A_i(N_i - n_i)n_c; \quad i = 1..4 \tag{1}$$

115 $$\frac{dm_j}{dt} = A_{mj}(M_j - m_j)m_v - \beta_j m_j n_c \; ; j = 1,2 \tag{2}$$

116 $$\frac{dn_c}{dt} = R + \sum_{i=1}^{4}\left[f\sigma_i n_i - A_i(N_i - n_i)n_c + s_i \exp\left(\frac{-E_i}{kT}\right) n_i \right] - \sum_{j=1}^{2} \beta_j m_j n_j \tag{3}$$

117 $$\frac{dm_v}{dt} = R - \sum_{j=1}^{2} A_{mj}(M_j - m_j)m_v \tag{4}$$

118 $$\sum_{j=1}^{2} m_j + m_v = \sum_{i=1}^{4} n_i + n_c \tag{5}$$

where n_i (cm^{-3}) and N_i (cm^{-3}), i=1…4, are the concentrations of trapped electrons and the concentrations of traps, respectively, m_j (cm^{-3}) and M_j (cm^{-3}), j=1,2, are the concentrations of holes trapped in recombination centres and the concentration of these centres, n_c (cm^{-3}) and m_v (cm^{-3}) are the concentrations of free electrons and holes in the conduction and valence bands, respectively, A_i (cm^3s^{-1}), i=1…4, are the probability coefficients of electron trapping in the corresponding traps, A_{mj} (cm^3s^{-1}), j=1,2, are the probability coefficients of hole trapping in the adequate recombination centres, *R* ($cm^{-3}s^{-1}$) is the intensity of the excitation irradiation producing the pairs of free electron and holes (taken as 10^{10} cm^3s^{-1} during the excitation process and 0 during bleaching), β_i (cm^3s^{-1}) are the probability coefficients of a free electron recombining with a hole trapped in the corresponding recombination centre (hereinafter referred to as recombination coefficient). The time-dependent probability of release of electrons from the i-th trap to the conduction band is equal $\gamma_i = \sigma_i f$, where σ_i (cm^2) is the optical cross-section of i-th trap and f ($cm^{-2}s^{-1}$) is the stimulation photon flux density (during excitation f=0). The probability of thermal release of electrons from the i-th trap to conduction band is equal $s_i \exp(-E_i/kT)$, where E_i and s_i are the thermal depth and the frequency factor of the i-th trap, respectively.

The concentration N_4 and the probability coefficient of electron trapping in disconnected traps, A_4 the concentrations of recombination centres M_j, the probability coefficient of a free electron recombining with a hole trapped in the luminescence centre β_i, were changed to check their impact on the dependence of the residual level on the total dose which was previously absorbed. Unless otherwise specified, the parameters of the model used in simulations are: $N_1=1.5\times10^7$ cm^{-3}, $N_2=10^9$ cm^{-3}, $N_3=2.5\times10^8$ cm^{-3}, $N_4=5\times10^{10}$ cm^{-3}, $M_1=M_2=10^{11}$ cm^{-3}, $A_1=10^{-8}$ cm^3s^{-1}, $A_2=10^{-9}$ cm^3s^{-1}, $A_3=5\times10^{-10}$ cm^3s^{-1}, $A_4=10^{-10}$ cm^3s^{-1}, $A_{m1}=A_{m2}=10^{-9}$ cm^3s^{-1}, $\beta_1=\beta_2=10^{-10}$ cm^3s^{-1}, $f=10^{15}$ $cm^{-2}s^{-1}$, $\sigma_1=1{,}96\times10^{-15}$ cm^2, $\sigma_2=2{,}22\times10^{-17}$ cm^2, $\sigma_3=5{,}41\times10^{-18}$ cm^2, E1=0,97 eV, E_2=1,7 eV, E_3=1,72 eV, $s_1 = 5\times10^{12}$ s^{-1}, $s_2 = 5\times10^{13}$ s^{-1}, $s_3 = 5\times10^{14}$ s^{-1}, T=293 K.

The model used in the simulations was constructed so that, while maintaining the greatest possible simplicity, it reproduces the degree of complication of the examined processes in real

materials, especially in natural materials such as minerals. The values of individual parameters were taken from the work by Bailey (2001) on the model of luminescence in quartz. It should be emphasized that such parameters for quartz as recombination coefficients or centers concentrations are not strictly defined. What is more, in subsequent works presenting the model for quartz (Adamiec et al., 2004, 2006; Bailey and Arnold, 2006; Adamiec et al., 2008; Pagonis et al., 2014; Friedrich et al., 2017), their different values appear, allowing the correct reproduction of the effects observed in this material. Here, we selected one of many possible sets of centres parameters. In order to demonstrate the effects related to the dependence of RHC on the total absorbed dose, not so much the precise absolute values of these parameters are essential, but the mutual ratios of these values, especially the concentrations of centres and recombination coefficients. The particular values of both kinds of parameters can fluctuate from sample to sample because of the various crystal lattice defects present in the materials of different origins.

During simulations, the concentration of holes in both recombination centres m_1 and m_2 was monitored after the optical bleaching. These values will be hereafter referred to as residual hole concentrations (RHC). Their values were observed for different duration of the irradiation with the intensity of the excitation (i.e. irradiation) producing pairs of free electrons and holes R equal to 10^{10} $cm^{-3}s^{-1}$. Simulation results, for the sake of clarity of presentation, are shown in the form of a dose dependence. The dose axis for all the results is directly related to the excitation time. It should be mentioned that several series of simulations were repeated for smaller R values, among them also values smaller by 6 orders of magnitude being chosen. When it can be assumed that one Gray generates about 1.5 x 10^7 electron-hole pairs in 1 cm^3 of quartz (Chen et al., 2020) the range of R value from 10^{10} $cm^{-3}s^{-1}$ to 10^4 $cm^{-3}s^{-1}$ corresponds to the dose rates ranging from 600 Gys^{-1} to 6 $mGys^{-1}$. Such a range of dose rates was tested in the simulations and no differences in the shape of RHC dependency on the dose were found for various dose rates. At the initial step of the simulations, different times of bleaching were tested. The bleaching time of 1000 s was found to be sufficient to effectively depopulate the optically active traps and was used in all the further simulations. For the

simulation results presented, the dependences of electron and hole concentrations on dose are shown for selected cases (panel a in the most of figures). They illustrate how the centres are filled during irradiation for various sets of model parameters.

3. Results

3.1. Significance of the presence of the disconnected trap.

First the dependence of the residual hole concentration on the concentration, N_4, and the coefficient of trapping probability, A_4, of disconnected traps was investigated. For this purpose, the concentrations of recombination centres as well as their recombination coefficients were fixed and set equal for both centres, $M_1 = M_2$ and $\beta_1 = \beta_2$, respectively. It is intuitively to foresee that the greater the dose at which the saturation level of occupation of these traps is achieved the bigger is also the dose at which the residual hole concentration in recombination centres after bleaching stabilises. Both parameters N_4 and A_4 control the rate at which the maximum filling of these traps is attained, so both are responsible for the shape of the dose dependence obtained for the residual

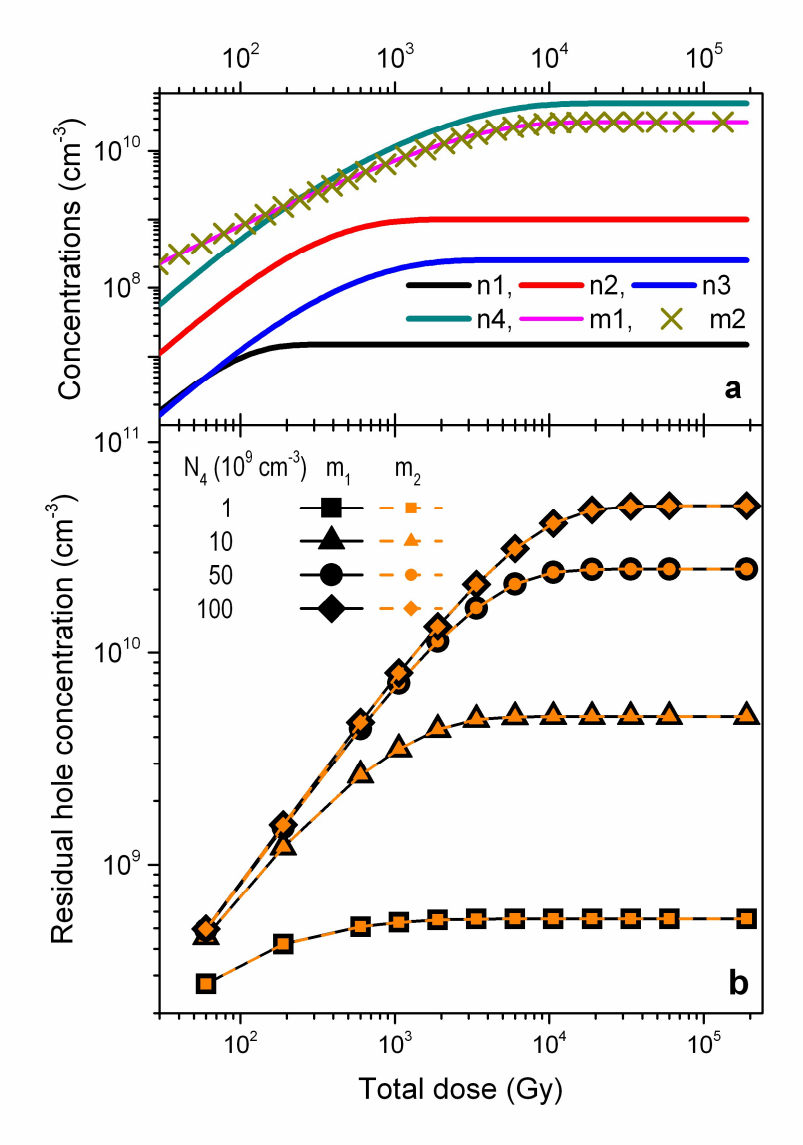

Fig. 2. Results of simulations for recombination centres having equal concentrations ($M_1 = M_2 = 10^{11}$ cm^{-3}) and recombination coefficients ($\beta_1 = \beta_2 = 10^{-10}$ cm^{3}s^{-1}) for different values of the concentration of disconnected traps. (a) - An example of growth curves for the electron and the hole concentrations, respectively, in traps and recombination centres for the case when concentration of disconnected traps $N_4 = 5\text{x}10^{10}$ cm^{-3}; (b) - The dependence of RHC after total emptying of shallower traps by optical stimulation for 1000 s on the total dose which was previously absorbed for four different values of N_4.

185 hole concentration. The first parameter only determines the final saturation value of the residual
186 hole concentration, because, as charge neutrality dictates, the number of holes trapped in both
187 recombination centres is equal to number of electrons in the disconnected traps. This is confirmed

188 by the results presented in Fig. 2 that show the dependency of the residual hole concentration in
189 both recombination centres after total emptying of shallower traps by optical stimulation for 1000 s
190 for four different values of disconnected trap concentration N_4 and the same A_4 value. The residual
191 hole concentration reaches its final saturation value for higher and higher doses as the concentration
192 of disconnected traps increases.

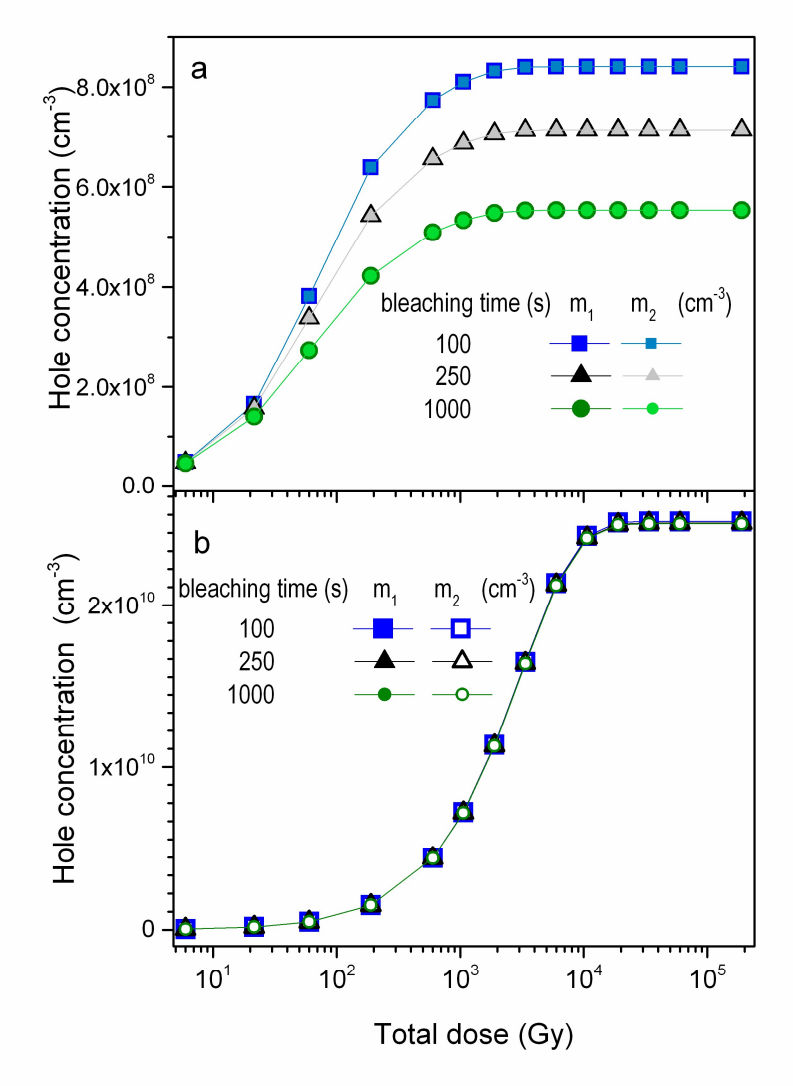

Fig. 3. The dependence of hole concentrations in the both recombination centres ($M_1 = M_2 = 10^{11}$ cm^{-3}, $\beta_1 = \beta_2 = 10^{-10}$ cm^3s^{-1}) on the total dose for different times of bleaching and two different concentrations of disconnected traps: (a) $N_4 = 10^9$ cm^{-3}; (b) $N_4 = 5 \times 10^{10}$ cm^{-3}. The concentrations of optically active traps are: $N_2=10^9$ cm^{-3} and $N_3=2.5x10^8$ cm^{-3}.

It is interesting to notice that the extent of changes of the concentration of holes in the recombination centres with the time of optical bleaching reflects the general relation of the concentration of optically active traps to the concentration of the disconnected traps. When the concentration of the latter has overwhelming majority over the concentration of bleachable traps the differences between the hole concentrations for different bleaching times are hardly noticeable. This is illustrated in Fig. 3b. In Fig. 3a, the differences in the hole concentrations for various bleaching times can be clearly observed, because the concentration of the disconnected trap is comparable with the concentrations of optically emptied traps. Such observations can be used for a qualitative assessment of the proportion of the concentration of the both kinds of traps.

For a defined concentration of disconnected traps, the coefficient of probability of electron trapping, A_4, dictates the rate of filling these traps. Therefore, its influence on the dose characteristics of residual hole concentration is easy to predict. The saturation level for different values of A_4, and fixed concentrations of the centres, stays the same but it is reached for progressively lower doses when A_4 increases. Such an effect is illustrated in Fig. 4 that shows the changes of residual hole concentration level in the recombination centres with dose. When the A_4 is equal to 10^{-11} cm^3s^{-1}, the residual hole concentration saturates for doses larger than 100 kGy, while for the trapping probability coefficient equal to 10^{-9} cm^3s^{-1} saturation starts around 5 kGy. Changes in the dose range for which the saturation of residual hole concentration occurs are dynamic when the A_4 is smaller than the trapping probability coefficients for the main optically active traps (A_2=10^{-9} cm^3s^{-1}, A_3=$5x10^{-10}cm^3s^{-1}$, see in Fig. 4b the curves for A_4= $0.1x10^{-10}cm^3s^{-1}$and $10^{-10}cm^3s^{-1}$). For the higher A_4 values, comparable with A_2 and A_3, ranging from 10^{-10} cm^3s^{-1} to 10^{-9} cm^3s^{-1}, the saturation range of residual hole concentration does not significantly change. It stabilizes when A_4 is comparable with the larger coefficient of the optically active traps, i.e. in this case A_2 = 10^{-9} cm^3s^{-1}.

The simulations presented in Fig. 4 were made for different concentrations of the recombination centres, M_1 = 10^{11} cm^{-3} and M_2 = 4×10^{10} cm^{-3}. Such cases are considered in detail

in subsection 3.2.2. Here, it is used to demonstrate that the dose at which the residual level reaches its final saturation level does not depend on the mutual relation of recombination centre concentrations. The factors that control this are the parameters of disconnected traps N_4 and A_4.

3.2. Influence of the properties of recombination centres.

As it can be clearly seen in Fig. 2, the maximum residual hole concentration as function of previous given dose depends on the relation of the concentration of disconnected traps N_4 to the concentrations of recombination centres. However, Fig. 2 presents simulation results for an exceptional case when both recombination centres have the same concentrations ($M_1 = M_2$) and recombination coefficients ($\beta_1 = \beta_2$). While for different samples of the same material the concentrations of specific defects (here M_1 and M_2) may be different, the recombination coefficients of these defects (here β_1 and β_2) remain constant from sample to sample. When one knows the recombination coefficient values of specific centres in the crystal, which is not the case with quartz, changes in RHC may be considered only regarding to different concentrations of recombination centres. So, it is interesting to observe how these different parameters individually affect the residual hole concentrations in recombination centres.

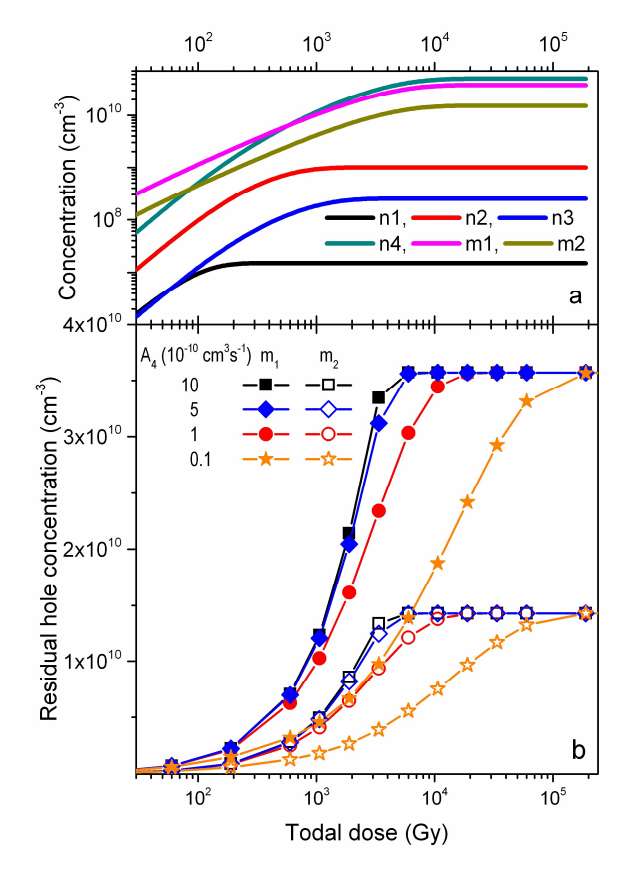

Fig. 4. Results of simulations for recombination centres having equal recombination coefficients ($\beta_1 = \beta_2 = 10^{-10}$ cm^{3}s^{-1}) and concentrations respectively: $M_1 = 10^{11}$ cm^{-3} and $M_2 = 4 \times 10^{10}$ cm^{-3}, for different values of the coefficient of probability of electron trapping in disconnected traps A_4. (a) - An example of growth curves for the electron and the hole concentrations in traps and recombination centres for the case when coefficient $A_4 = 10^{-10}$ cm^{3}s^{-1}; (b) - The dependence of RHC on the total dose which was previously absorbed for four different values of A_4. The concentration of disconnected traps is set to $N_4 = 5 \times 10^{10}$ cm^{-3}.

3.2.1 The impact of recombination coefficients of the centres on the residual hole concentration

First the simulation was conducted for equal concentrations M_1 and M_2 and different relations between the recombination coefficients β_1 and β_2 were tested with the fixed assumption that $\beta_1 > \beta_2$. An interesting effect can be noticed in Fig. 5, which shows the results for a wide range of β_2 values and β_1 equal to 10^{-10} cm^{3}s^{-1}. When β_1 is greater than β_2 but no more than four times (5×10^{-11}, 7.5×10^{-11} cm^{3}s^{-1}) the dependence of the residual hole concentration on dose is similar in shape to

all the curves presented previously in Figs 2 - 5. For lower β_2 values (in Fig. 5 for $\beta_2 = 0.5 \times 10^{-11}$, 10^{-11}, $2.5 \times 10^{-11} cm^3 s^{-1}$), in the case of the recombination centre number 1 with the greater recombination coefficient β_1, a peak is observed before the dependence of residual hole concentration on dose reaches its stable final level. The amplitude of this peak depends on the relationship between the concentrations of recombination centres M_1 and M_2 which will be shown in subsection 3.2.2. The ratio β_1/β_2, instead, decides about the final saturation value of the residual hole concentration for doses higher that those causing the peak. For a fixed M_1/M_2 ratio, the level is the lower the greater the difference between the two coefficients and reaches zero for extreme cases, here for $\beta_1/\beta_2 = 20$.

It is important to notice that the peak similar to that observed in the dependence of RHC on the total dose appears also in the growth curves of hole concentration of the respective recombination centre (see Fig. 5a). This is the consequence of the fact that the recombination rate is controlled not only by the recombination coefficient (β_1 and β_2) but also by the current hole concentration m_1 and m_2. The terms in the kinetics equations responsible for recombination rates are $\beta_1 m_1 n_c$ and $\beta_2 m_2 n_c$ which shows that both processes are also coupled by the current state of electron concentration in the conduction band described by the Eq. (3) and compete with each other. For low β_2 and m_2, the rate of recombination at centre 2 is simply lower than at centre 1 which although catches the holes during irradiation simultaneously loses them more effectively. When all the traps are almost full, the electrons in the conduction band have are less effectively trapped and then the recombination process at centre 1 becomes the most effective way for their relaxation. That leads to lower hole concentration in this recombination centre after irradiation and then also to the lower RHC values after bleaching.

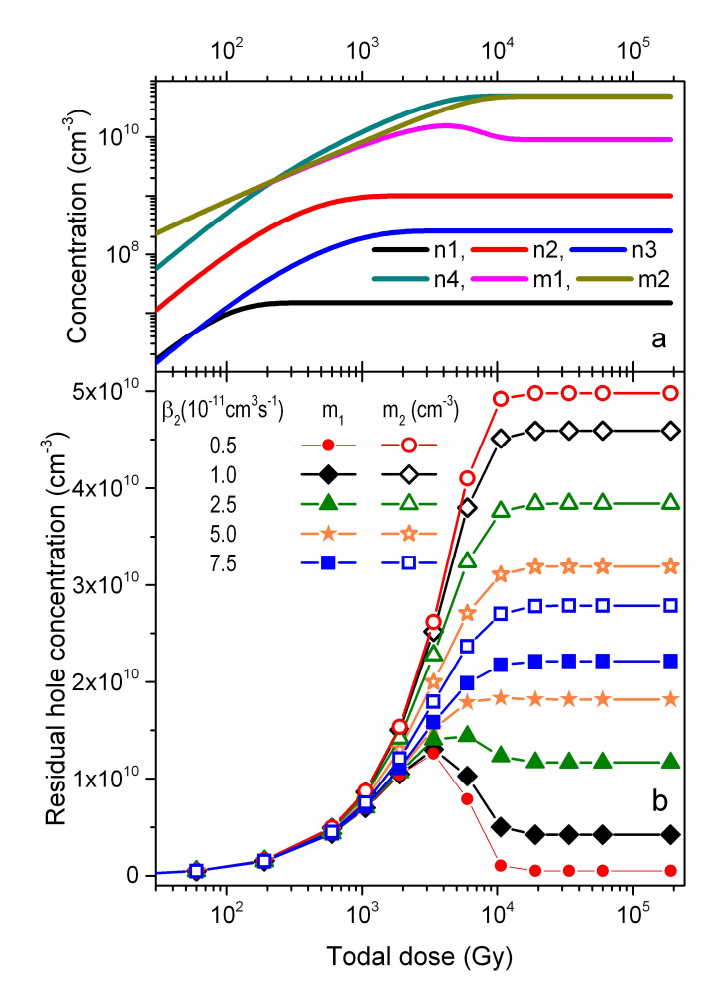

Fig. 5. Results of simulations for recombination centres having equal concentrations ($M_1 = M_2 = 10^{11}$ cm^{-3}) and different values of the recombination coefficients β_1 and β_2. β_1 is fixed and equal to 10^{-10} cm^{3}s^{-1}, when β_2 is changed. (a) - An example of growth curves for the electron and the hole concentrations in traps and recombination centres for the case when the recombination coefficient $\beta_2 = 10^{-11}$ cm^{3}s^{-1}; (b) - The dependence of RHC on the total dose which was previously absorbed for five different values of β_2. The concentration of disconnected traps is set to $N_4 = 5 \times 10^{10}$ cm^{-3}.

The value of β_1/β_2 ratio for which the peak in the dose dependence of residual hole concentration appears is controlled by the relation of recombination centres concentrations M_1 and M_2 to the concentration of disconnected traps. When both M_1 and M_2 are significantly bigger than N_4 the peak is always observed for $\beta_1 > 2\beta_2$. For close values of the concentrations of recombination centres and disconnected traps the difference between β_1 and β_2 has to be bigger. The effect is

illustrated by Fig. 6 which is a repetition of the simulations presented in Fig. 5 but with two different concentrations of recombination centres M_1 and M_2. In Fig 6a and c $M_1 = M_2$ and is twice than the values chosen in Fig. 5 , while in Fig. 6c and d the value is a much smaller equal to N_4 . As can be seen for example for $\beta_2 = 10^{-11}$ or $2.5 \times 10^{-11} cm^3 s^{-1}$ in Fig. 6a, the final saturation value, in other words the stabilization level for the residual hole concentration is clearly lower for bigger M_1 and M_2 (equal to $2x10^{11} cm^{-3}$) and for $\beta_2 = 5 \times 10^{-11} cm^3 s^{-1}$ the slight decrease after approaching the maximum value of hole concentration may be noticed. The latter was not present for lower M_1 and M_2 ($10^{11} cm^{-3}$) on Fig. 5. When M_1 and M_2 are close to the concentration of disconnected traps (Fig. 6b, all equal to $5x10^{10} cm^{-3}$), the decrease of the dose dependence curve after reaching the maximum value can be hardly noticed for $\beta_2 = 2.5 \times 10^{-11} cm^3 s^{-1}$ for which the decrease is clearly visible in Fig. 5. The very low value of final saturation value, close to zero, seen for the smaller value of β_2 (0.5×10^{-11} $cm^3 s^{-1}$) in Fig. 5 and Fig. 6b is not observed here.

It is also worth noting that the amplitudes of the peaks observed in the dose dependence curves presented in Fig. 5 and 6 does not change. Additionally, it was checked that as long as the M_1/M_2 ratio does not change, the concentrations M_1 and M_2 alone have no effect on the peak height of the dose dependence of the residual hole centres. A corresponding result of simulations are presented in Fig. S1 in Supplementary Materials. This is because, as was mentioned above, it is the M_1/M_2 ratio that dictates the amplitude of the peak. Here, it can be also observed that in the case when M_1 and M_2 are smaller than N_4 the peak in the dose dependence curve is not observed (Fig. S1, curve for $M_1 = M_2 = 2.5 \times 10^{10} cm^{-3}$).

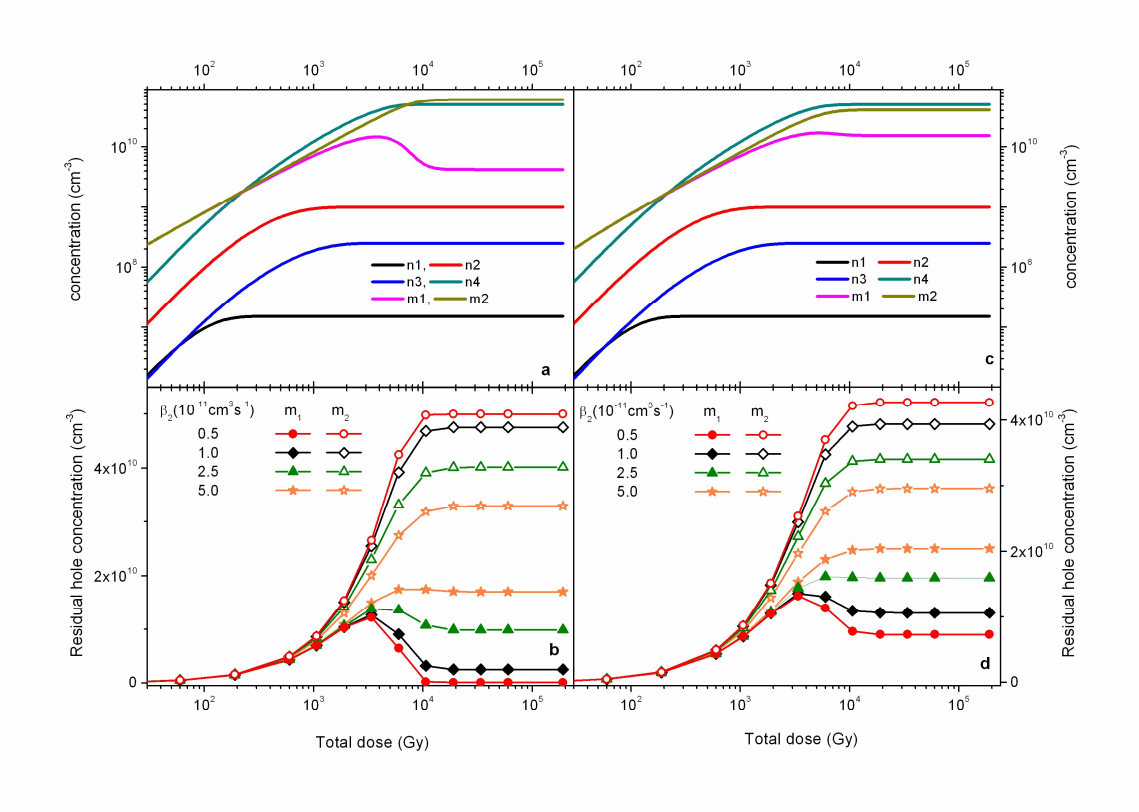

Fig. 6. Results of simulations for recombination centres having equal concentrations and different values of the recombination coefficients β_1 and β_2. β_1 is fixed and equal to 10^{-10} cm^3s^{-1}, when β_2 is changed. (a) - An example of growth curves for the electron and the hole concentrations in traps and recombination centres for the case when their concentrations are $M_1 = M_2 = 2 \times 10^{11}$ cm^{-3} and recombination coefficient $\beta_2 = 5 \times 10^{-10}$ cm^3s^{-1}; (b) - The dependence of RHC on the total dose which was previously absorbed for five different values of β_2 when $M_1 = M_2 = 2 \times 10^{11}$ cm^{-3}; (c) - An example of growth curves for the electron and the hole concentrations in traps and recombination centres for the case when their concentrations are $M_1 = M_2 = 5 \times 10^{10}$ cm^{-3} and recombination coefficient $\beta_2 = 10^{-11}$ cm^3s^{-1}; (d) - The dependence of RHC on the total dose for five different values of β_2 when $M_1 = M_2 = 5 \times 10^{10}$ cm^{-3}. The concentration of disconnected traps is $N_4 = 5 \times 10^{10}$ cm^{-3}.

3.2.2. The influence of the concentrations of the recombination centres on the residual hole concentration

To investigate the influence of the concentration of the recombination centres on the changes of residual hole concentrations with dose the β_1/β_2 ratio and the concentration of disconnected traps N_4 were established and the processes were modelled for different relationships between M_1 and

293 M_2. Fig. 7 shows the residual hole concentrations after emptying the optically sensitive traps versus
294 the dose. As the β_1/β_2 ratio is set to 10 the peak can be observed for every case. The greater the M_1 /
295 M_2 ratio the higher is the peak in the dose dependence for the recombination centre 1. It was
296 checked that for fixed M_1 / M_2 ratio the individual values of recombination centre concentrations
297 play here a minor role. The results illustrating this are shown in Supplementary Material in Fig. S2.

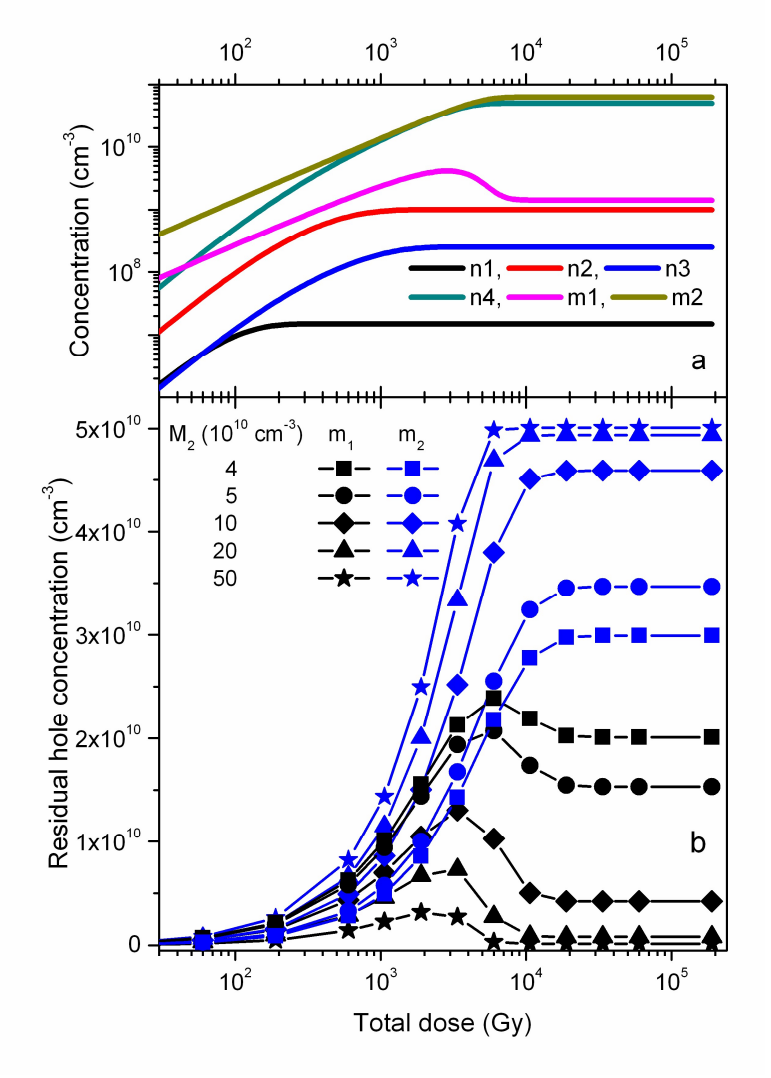

Fig. 7. Results of simulations for recombination centres for fixed recombination coefficients : $\beta_1 = 10^{-10}$ cm^3s^{-1}, $\beta_2 = 10^{-11}$ cm^3s^{-1} and various ratios of the recombination centre concentrations M_1/M_2. M_1 is always equal to 10^{11} cm^{-3} and the value of M_2 is changed, $N_4 = 5 \times 10^{10}$ cm^{-3}. (a) - An example of growth curves for the electron and the hole concentrations in traps and recombination centres for the case when the recombination centre concentration $M_2 = 5x10^{11}$ cm^{-3}; (b) - The dependence of RHC on the total dose which was previously absorbed for five different values of M_2.

In Fig. 7, an interesting detail can be noticed. The stabilization level of residual hole concentration is attained for lower doses when concentration M_2 increases. This indicates that not only the concentration of disconnected traps dictates the dose range where residual hole concentration stabilization occurs but also, in the second order, its relation to the sum of concentrations of recombination centres ($M_1 + M_2$).

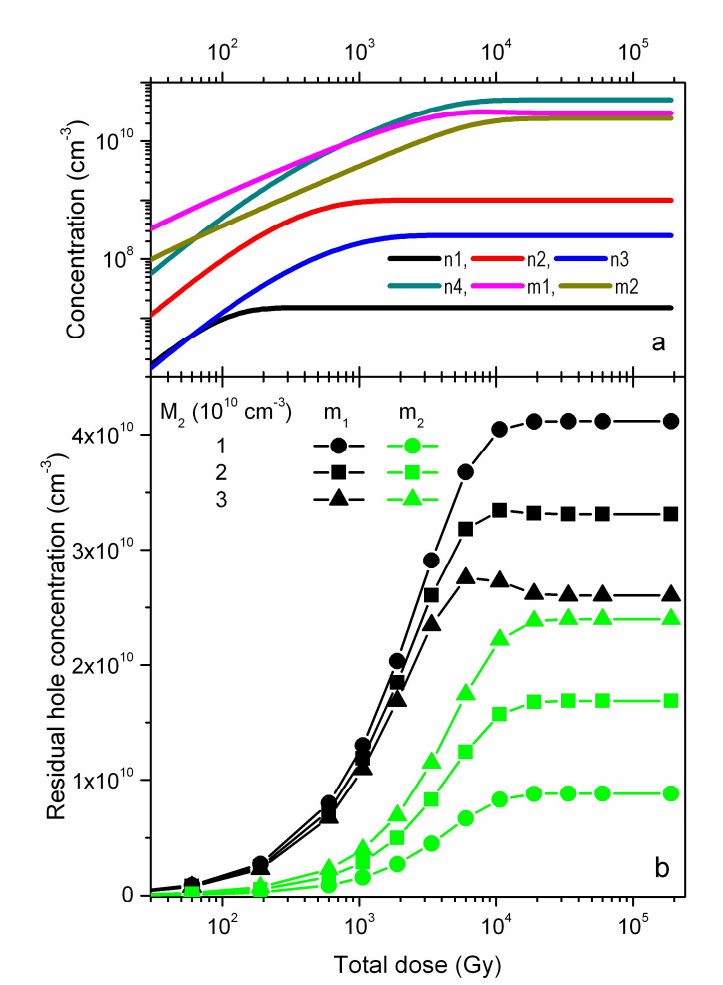

Fig. 8. Results of simulations for recombination centres for selected cases when the concentration M_2 of recombination centre with the lower recombination coefficient is smaller than the concentration of the disconnected traps $N_4 = 5 \times 10^{10}$ cm^{-3}. The recombination coefficients : $\beta_1 = 10^{-10}$ cm^{3}s^{-1}, $\beta_2 = 10^{-11}$ cm^{3}s^{-1} and the concentration $M_1 = 10^{11}$ cm^{-3}. (a) - An example of growth curves for the electron and the hole concentrations in traps and recombination centres for the case when the recombination centre concentration $M_2 = 3 \times 10^{10}$ cm^{-3}; (b) - The dependence of RHC on the total dose for three different values of M_2.

As it was already noticed above, the peak in the dose dependence of the residual hole concentration does not occur when $M_1 = M_2 < N_4$. However, when only one of the recombination centres has the concentration lower than N_4, the peak appears. A good example is the dose dependence shown in Fig. 7 for $M_2 = 4 \times 10^{10}$ cm^{-3}. But it was also observed that for small enough concentration of M_2, the peak in the dose dependency curve disappears and additionally the relation between the final saturation values of RHC of both centres is changed. When for larger M_2, the residual hole concentrations for recombination centre 2 saturates for larger values than for recombination centre 1, for very small M_2 this is reversed, and the bigger saturation value is observed for centre 1. Both effects are presented in Fig. 8 for various M_2 values. For very low M_2, the hole trapping at this centre is very slow and because of that the hole concentration in this centre is continuously lower than hole concentration in centre 1, which can be observed for both the hole concentrations during irradiation as well as residual hole concentrations in Fig. 8. This makes the recombination centre 2 "hardly visible" for the processes taking place at the centre 1 and unable to compete effectively. This makes that the peak in the dose dependence curves, which is a result of competition between the recombination processes in both centres, is vanishing with decreasing M_2 values. When the dose range for which the stabilization of residual levels occurs is reached, recombination centre 2 stays completely filled out after the bleaching and centre 1 ensures the fulfilment of electric charge neutrality.

4. Discussion

ESR is a very powerful experimental tool for the detection and identification of defects in solid states (Lund and Shiotani, 2014). As such it is also a perfect tool for measuring the trapped charge concentration based on which ages are determined in ESR dating (Grün, 2020; Rizal et al, 2020). However, for accurate applications to be carried out the initial concentration of charge at the moment that is considered the starting point for time measurement needs to be known. The most convenient and desirable situation is the lack of charge in the traps at this initial moment. The

329 complexity of charge transport processes in crystals, and especially in natural crystals, makes one
330 doubt this state is always possible, especially when the ESR signal is resetted by light exposure. When
331 the measurement of such initial concentration gives a negligible result in comparison to the
332 concentrations measured to determine the age this assumption is likely valid.

333 For Al-hole signals however, it is well known this is not the case, and generally a value which is
334 not negligible is determined and taken into account in the age estimation by adequately reducing the
335 value obtained by the application of dating protocols (e.g. Voinchet et al., 2003). There is, however,
336 one necessary condition for such corrections to be valid, and that is that the residual value obtained
337 by laboratory measurements has to agree with the initial natural value at the start point for time
338 measurement. The results presented here clearly show that this cannot usually be the case when the
339 concentration of holes in recombination centres is used for age estimation and the factor responsible
340 for the ESR signal zeroing is light. The ESR measurement results for quartz extracted from sediments
341 clearly presented that the residual level of the ESR signal related to Al centre in quartz depends on
342 the total dose absorbed in quartz before the beaching (Timar-Gabor et al., 2020). The nature of this
343 dependence is a consequence of the rule of electric charge neutrality and the complex processes of
344 charge transfer in the crystal. These processes are controlled by the physical parameters of the
345 centres involved: the probability coefficients of electron or hole trapping in the corresponding trap
346 and the recombination coefficients of a free electron recombination with a hole trapped in the
347 recombination centre, as well as by the concentrations of the centres which are expected to vary
348 from sample to sample.

349 We have investigated these effects using the band gap model by considering four electron
350 traps and two recombination centres. It should be noted that although only one kind of disconnected
351 trap type was considered, it stands for the many kinds typically found in quartz. The sum of their
352 concentrations may well exceed the concentration of the optically emptied traps. The presented
353 results seem to indicate a favourable case, which could allow the use of ESR signal from the Al-hole
354 centre in quartz for sediment dating without the risk that the RHC level included in the age

355 calculation does not correspond to the real one. It is when the concentration of disconnected traps is
356 low compared to the concentration of optically emptied traps, as this makes the overall RHC levels
357 low compared to the hole concentration in recombination centres immediately after excitation. In
358 this case the difference between the ESR intensity of the natural sample at the moment of bleaching
359 and that of the laboratory bleached sample will be negligible. Another case that may also lead to
360 same small values of the difference between the ESR intensity of Al-hole centre of the natural sample
361 and that of the laboratory bleached one is quartz containing a recombination centre with a much
362 higher concentration and a several times lower recombination coefficient than the Al-hole centre.
363 Then the residual hole concentration for a centre of low concentration (here by assumption Al-hole
364 centre) has mostly low levels and stabilizes at a value close to zero. Such a case is illustrated by the
365 dose dependence curves presented in Fig. 7 for M_2= 2 x 10^{11} cm^{-3} or 5 x 10^{11} cm^{-3}. The concentration
366 of centre 1 is M_1= 10^{11} cm^{-3} , which is, two or five times less than the concentration of centre 2. Other
367 similar cases are presented in Supplementary Material in Fig. S2. However, it is hard to assume that
368 Al-hole centre plays the role of centre 1 in such cases because it is very unlikely that there will be a
369 centre in quartz having a higher concentration. Other ions occur in quartz in concentrations on
370 average ten times lower than Al. The latter occurs in high concentrations (up to a few 1000 ppm,
371 Müller et al., 2003, 2012) due to the common occurrence of Al in the Earth crust and the similarity of
372 ionic radius of Si^{4+} and Al^{3+}. Because of the above Al may be regarded as the recombination centre
373 with potentially the highest concentration. In this case significant and variable residual hole
374 concentrations can be expected for Al-hole centre. This seems to be confirmed by practice as usually
375 high values are reported in the literature for the relative difference between the ESR intensity of the
376 natural sample used for equivalent dose determination and that of the signal after laboratory
377 bleaching the natural samples in the laboratory. For example, Walther and Zilles (1994) reported a
378 residual level at 44% of the natural, Voincet et al. (2003) reported a maximum bleached value of 50 %
379 of the natural, Rink et al. (2007) observed that the remaining signal was 56% of the natural ESR
380 intensity measured prior to light exposure., while Voinchet et al. (2015) examined modern samples

381 from various sedimentary environments (fluvial, marine and aeolian) and reported bleaching rates
382 (expressed as % of the total signal that can be bleached) of up to 22%.

383 Due to the lack of data on the recombination coefficient of Al-hole centre two opposite cases
384 should be taken into account: (1) when this coefficient is bigger than for other centres and (2) when
385 another centre with a bigger recombination coefficient than of Al-hole centre exists.

386 In the first case, a complex dose dependence for the residual hole concentration after
387 bleaching may be expected. The possible changes of the residual hole concentration with dose can
388 be seen in Fig. 6 for different ratios of the probability coefficients of both centres and two different
389 relations of the recombination centre concentrations to the disconnected trap concentration. The Al-
390 hole centre plays here the role of centre 1. The shape of dose dependency curves for this centre (m_1)
391 varies between a function which monotonically increases up to a stabilization level and a peak shape
392 curve. The relative fluctuations in residual hole concentration with the total dose are the most
393 significant for big differences between recombination coefficients (e.g. curves for $\beta_2 = 2.5 \times 10^{-11}$ cm^3
394 s^{-1} and 5×10^{-11} cm^3 s^{-1}, when $\beta_2 = 10^{-10}$ cm^3 s^{-1}), because after the peak very low values are reached in
395 the stabilization range. So a very low residual hole concentration observed for old samples could find
396 explanation by the conceivable large predominance of the recombination coefficient of Al centre
397 over the coefficients of the rest of recombination centres. It may also explain why in some cases the
398 results obtained by signals from the Ti and Al-hole centres in the quartz are consistent (Tissoux, et al.,
399 2007, Bartz et al., 2018; Duval et al., 2020; Bahain et al., 2020; Bartz et al., 2020), and in others they
400 are not (Duval and Guilarte, 2015; Duval et al., 2017; Demuro et al., 2020). Sometimes the residual
401 hole concentration for the Al centre is close to zero (Tissoux, et al., 2012). However, such a case does
402 not necessarily mean that the ESR signal of Al-hole centre was also close to zero in result of bleaching
403 during the deposition process of the quartz grains. In case when Al-hole centre has the biggest
404 recombination coefficient from all centres, significantly higher RHC could appear for lower total
405 absorbed doses (e.g. Fig. 7, curve for $\beta_2 = 10^{-11}$ and 5×10^{-12} cm^3 s^{-1}). At this point, it is important to
406 note that the complex peak shape is observed also in the growth curves of the hole concentration in

recombination centres with the high recombination coefficient. This can be seen in parts a of Figs 5 - 7. The second case, when another centre has the bigger recombination coefficient than Al-hole centre, does not lead to as much complex behavior of the dose dependence curve for the RHC. But still, the RHC changes with dose. The absolute value of the residual hole concentration strongly depends on the concentration and the probability coefficient of trapping of disconnected traps as can be observed in Fig. 2 and 4. Moreover, the same factors dictate the dose range where the residual hole concentration starts to stabilize. Therefore, also in the case when the Al-hole centre is not the recombination centre with the larger value of the recombination coefficient, the dose dependence of the residual hole concentration may explain a variety of the unbleachable residuals levels of ESR signal from Al-hole centre reported in the literature as well the observed strong sample dependency (e.g Toyoda et al., 2000, Tissoux et al., 2012; Duval et al., 2017, Bartz et al., 2020).

To sum up, regardless of the magnitude of the recombination coefficient of Al-hole centre, the residual concentration level of holes that is reached after the bleaching of the quartz grains is practically impossible to estimate. The first reason is that the total dose of radiation absorbed by the grains since their inception, more precisely from the moment when the disconnected traps were emptied, to the moment when grains were exposed to light is not known. The equivalent dose, the dose accrued after deposition until the moment of measurement is obviously not known as this is the measurable in the dating process. For this reason, even if the dose dependency of residual hole concentration could be well constrained by laboratory experiments, it is not possible to determine where on this dose dependency the point of sediment deposition lies on. The construction of natural dose response curves does not seem to fully solve the problem either, as one can easily see from the results above that it cannot be assumed that the RHC level was the same in all samples used to construct the curve. The dose dependence of the RHC is sample specific because it strongly depends on the concentration of all kinds of defects in quartz.

5. Conclusions

As long as the hole centres are believed to be disintegrated by light in the process of recombination of electrons from conduction band with holes in these centres, there is no reason to believe that the number of the residual hole centres that remain after the optical bleaching can be assumed to be constant and fixed from sample to sample. The detailed investigation of the possible levels of residual hole concentrations in recombination centres after the bleaching shows that they change with the total dose absorbed in the history of the sample. The character of the dose dependency may vary significantly from sample to sample. It is hard to reconstruct the shape of this dependency, and it is impossible to know the total dose accrued in the crystal before the bleaching event. Until one knows the relation of the recombination coefficient of the centre whose signal is used for dating (in the case of quartz is the Al-hole centre) to the recombination coefficients of the other recombination centres, one cannot assume that the RHC determined in the laboratory corresponds to the natural value.

Acknowledgement: Alida Timar-Gabor has received funding from the European Research Council (ERC) under the European Union's Horizon 2020 research and innovation programme ERC-2015-STG, (grant agreement No [678106]).

References

Adamiec, G., Garcia-Talavera, M., Bailey, R. M., De La Torre, P. I., 2004 . Application of a genetic algorithm to finding parameter values for numerical simulation of quartz luminescenc Geochronometria 23, 9-14.

Adamiec, G., Bluszcz, A., Bailey, R. M., Garcia-Talavera, M. 2006. Finding model parameters: Genetic algorithms and the numerical modelling of quartz luminescence. Radiation Measurements 41 (7-8), 897-902. 10.1016/j.radmeas.2006.05.005

458 Adamiec, G., Bailey, R. M., Wang, X. L., Wintle, A. G, 2008. The mechanism of thermally transferred
459 optically stimulated luminescence in quartz. Journal of Physics D: Applied Physics 41 (13), 135503.
460 stacks.iop.org/JPhysD/41/135503Aitken, M. J., 1998. An Introduction to Optical Dating, Oxford
461 University Press, Oxford.

462 Bahain, J. J., Duval, M., Voinchet, P., Tissoux, H., Falgu`eres, C., Grün, R., Moreno, D., Shao, Q.,
463 Tombret, O., Jamet, G., Faivre, J.-P., Cliquet, D., 2020. ESR and ESR/Useries chronology of the Middle
464 Pleistocene site of Tourville-la-Rivi`ere (Normandy, France) - a multi-laboratory approach. Quat. Int.
465 556, 58–70. https://doi.org/10.1016/j.quaint.2019.06.015

466 Bartz, M., Rixhon, G., Duval, M., King, G. E., ´Alvarez-Posada, C., Par´es, J. M., Brückner, H., 2018.
467 Successful combination of electron spin resonance, luminescence and palaeomagnetic dating
468 methods allows reconstructing the Quaternary evolution of the lower Moulouya River (NE Morocco).
469 Quat. Sci. Rev. 185, 153–171. https://doi.org/10.1016/j.quascirev.2017.11.008

470 Bartz, M., Duval, M., Brill, D., Zander, A., King, G. E., Rhein, A., Walk, J., Stauch, G., Lehmkuhl, F.,
471 Brückner, H., 2020. Testing the potential of K-feldspar pIR-IRSL and quartz ESR for dating coastal
472 alluvial fan complexes in arid environments. Quat. Int. 556, 124–143.
473 https://doi.org/10.1016/j.quaint.2020.03.037

474 Bailey R. M., 2001. Towards a general kinetic model for optically and thermally stimulated
475 luminescence of quartz. Radiation Measurements 32: 17-45. https://doi.org/10.1016/S1350-
476 4487(00)00100-1

477 Bailey, R.M., Arnold, L.J., 2006. Statistical modelling of single grain quartz De distributions and an
478 assessment of procedures for estimating burial dose. Quaternary Science Reviews 25, 2475–2502.
479 https://doi.org/10.1016/j.quascirev.2005.09.012

480 Chen, R., Lawless, J.L., Pagonis, V., 2020. Competition between long time excitation and fading of
481 thermoluminescence (TL) and optically stimulated luminescence (OSL), Radiation Measurements 136,
482 106422. https://doi.org/10.1016/j.radmeas.2020.106422

Chruścińska, A., Przegiętka, K. R., 2005. Quartz TL decay due to optical bleaching, Geochronometria 24, 1-6.

Demuro, M., Arnold, L. J., Duval, M., M´endez-Quintas, E., Santonja, M., P´erez- Gonz´alez, A., 2020. Refining the chronology of Acheulean deposits at Porto Maior in the River Miño basin (Galicia, Spain) using a comparative luminescence and ESR dating approach. Quat. Int. 556, 96–112. https://doi.org/10.1016/j.quaint.2020.01.005

Duval, M., Guilarte, V., 2015. ESR dosimetry of optically bleached quartz grains extracted from Plio-Quaternary sediment: evaluating some key aspects of the ESR signals associated to the Ti-centers. Radiat. Meas. 78, 28–41. https://doi.org/10.1016/j.radmeas.2014.10.002

Duval, M., Arnold, L. J., Guilarte, V., Demuro, M., Santonja, M., Perez-Gonzalez, A., 2017. Electron spin resonance dating of optically bleached quartz grains from the Middle Palaeolithic site of Cuesta de la Bajada (Spain) using the multiple centres approach. Quat. Geochronol. 37, 82–96. https://doi.org/10.1016/j.quageo.2016.09.006

Duval, M., Voinchet, P., Arnold, L.J., Par´es, J. M., Minnella, W., Guilarte, V., Demuro, M., Falgu`eres, C., Bahain, J.-J., Despri´ee, J., 2020. A multi-technique dating study of two lower palaeolithic sites from the cher valley (Middle loire catchment, France): lunery-la Terre-des-Sablons and brinay-la Noira. Quat. Int. 556, 71–87. https://doi.org/10.1016/j.quaint.2020.05.033

Friedrich, J., Kreutzer, S., Schmidt, C., 2016. Solving ordinary differential equations to understand luminescence: 'RLumModel', an advanced research tool for simulating luminescence in quartz using R , Quaternary Geochronology 35, 88-100. https://doi.org/10.1016/j.quageo.2016.05.004

Friedrich, J., Pagonis, V., Chen, R., Kreutzer, S., Schmidt, C., 2017. Quartz radiofluorescence: a modelling approach. Journal of Luminescence 186, 318-325. https://doi.org/10.1016/j.jlumin.2017.02.039

Grün, R., 2020. A very personal, 35 years long journey in ESR dating, Quat. Int. 556, 20-37. https://doi.org/10.1016/j.quaint.2018.11.038

508 Lund A., Shiotani M. (Eds.), 2014. Applications of EPR in Radiation Research, Springer Cham
509 Heidelberg New York Dordrecht London.

510 Müller, A., Wiedenbeck, M., van den Kerkhof, A. M., Kronz, A., Simon, K., 2003. Trace elements in
511 quartz — a combined electron microprobe, secondary ion mass spectrometry, laser-ablation ICP-MS,
512 and cathodoluminescence study. European Journal of Mineralogy 15 (4), 747–763.
513 DOI: 10.1127/0935-1221/2003/0015-0747

514 Müller, A., Wanvik J. E., Ihlen, P. M., 2012. Petrological and Chemical Characterisation of High-Purity
515 Quartz Deposits with Examples from Norway, in: Götze, J., Möckel, R. (Eds), Quartz: Deposits,
516 Mineralogy and Analytics, Springer-Verlag Berlin, pp. 71-118.

517 Pagonis, V., Chithambo, M.L., Chen, R., Chruścińska, A., Fasoli, M., Li, S. H., Martini, M., Ramseyer, K.,
518 2014. Thermal dependence of luminescence lifetimes and radioluminescence in quartz. Journal of
519 Luminescence 145, 38-48. https://doi.org/10.1016/j.jlumin.2013.07.022

520 Peng, J., Pagonis, V., 2016. Simulating comprehensive kinetic models for quartz luminescence using
521 the R program KMS, Radiation Measurements 86, 63-70.
522 https://doi.org/10.1016/j.radmeas.2016.01.022

523 Preusser, F., Chithambo, M. L., Götte, T., Martini, M., Ramseyer, K., Sendezera, E. J., Susino, G. J.,
524 Wintle, A. G., 2009, Quartz as a natural luminescence dosimeter, Earth-Science Reviews 97, 184–
525 214. https://doi.org/10.1016/j.earscirev.2009.09.006

526 Przegiętka, K. R., Richter, D., Chruścińska, A., Oczkowski, H. L., Lankauf, K. R., Szmańda, J. B., Luc, M.,
527 Chudziak, W., 2005. Quartz Luminescence Applied in Palaeoenvironmental Reconstruction of a Dune.
528 Physica Scripta 118, 257-260.

529 Rink, W. J, 1997. "Electron spin resonance (ESR) dating and ESR applications in quaternary science
530 and archaeometry". Radiat. Meas. 27 (5–6), 975–1025. https://doi.org/10.1016/S1350-
531 4487(97)00219-9

532 Rink, W.J., Bartoll, J., Schwarcz, H.P., Shane, P., Bar-Yosef, O., 2007. Testing the reliability of ESR
533 dating of optically exposed buried quartz sediments. Radiation Measurements 42, 1618-1626.
534 https://doi.org/10.1016/j.radmeas.2007.09.005

535 Rizal, Y., Westaway, K. E., Zaim, Y., van den Bergh, G. D., Bettis III, E. A., Morwood, M. J., Huffman, O.
536 F., Grün, R., Joannes-Boyau R., Bailey, R. M., Sidarto, Westaway, M. C., Kurniawan, I., Moore, M. W.,
537 Storey, M., Aziz, F., Suminto, Zhao, J., Aswan, Sipola, M. E., Larick, R., Zonneveld, J.-P., Scoot R., Putt,
538 S., Ciochon, R. L., 2020. Last appearance of Homo erectus at Ngandong, Java, 117,000-108,000 years
539 ago. Nature 577, 381-385. DOI: 10.1038/s41586-019-1863-2

540 Singhivi, A. K., Sharma, Y. P., Agrawal, P. D., 1982. Thermoluminescence dating of sand dunes in
541 Rajasthan, India. Nature 295, 313-315. https://doi.org/10.1038/295313a0

542 Smith, B. W., Rhodes, E. K., 1994. Charge movements in quartz and their relevance to optical dating.
543 Radiat. Meas. 23 (2-3), 329-333. https://doi.org/10.1016/1350-4487(94)90060-4

544 Spooner, N. A., 1994. On the optical dating signal from quartz. Radiat. Meas. 23 (2-3), 593-600.
545 https://doi.org/10.1016/1350-4487(94)90105-8

546 Timar-Gabor, A., Chruścińska, A., Benzid, K., Fitzsimmons, K. E., Begy, R., Bailey, M., 2020. Bleaching
547 studies on Al-hole ([AlO4/h]0) electron spin resonance (ESR) signal in sedimentary quartz. Radiat.
548 Meas. 130, 106-221. https://doi.org/10.1016/j.radmeas.2019.106221

549 Tissoux, H., Voinchet, P., Lacquement, F., Prognon, F., Moreno, D., Falguères, Ch., ,Bahain, J.-J.,
550 Toyoda, S., 2012. Investigation on non-optically bleachable components of ESR aluminium signal in
551 quartz. Radiat. Meas. 47 (9), 894–899. https://doi.org/10.1016/j.radmeas.2012.03.012

552 Toyoda, S., Voinchet, P., Falguéres, C., Dolo, J. M., Laurent, M., 2000. Bleaching of ESR signals by the
553 sunlight: a laboratory experiment for establishing the ESR dating of sediments. Appl. Radiat. Isot. 52
554 (5), 1357–1362. https://doi.org/10.1016/S0969-8043(00)00095-6

555 Toyoda, S., Falguéres, C., 2003. The method to represent the ESR signal intensity of the aluminium
556 hole center in quartz for the purpose of dating. Adv. ESR Appl. 201, 7–10.

557 Tsukamoto, S., Porat, N., Ankjærgaard, C., 2017. Dose recovery and residual dose of quartz ESR
558 signals using modern sediments: implications for single aliquot ESR dating. Radiat. Meas. 106, 472–
559 476. https://doi.org/10.1016/j.radmeas.2017.02.010

560 Tsukamoto, S., Long, H., Richter, M., Li, Y., King, G. E., He, Z., Yang, L., Zhang, J., Lambert, R., 2018.
561 Quartz natural and laboratory ESR dose response curves: a first attempt from Chinese loess. Radiat.
562 Meas. 120, 137–142. https://doi.org/10.1016/j.radmeas.2018.09.008

563 Voinchet, P., Falguéres, C., Laurent, M., Toyoda, S., Bahain, J.J., Dolo, J.M., 2003. Artificial optical
564 bleaching of the Aluminium center in quartz implications to ESR dating of sediments. Quat. Sci. Rev.
565 22, 1335–1338. https://doi.org/10.1016/S0277-3791(03)00062-3

566 Voinchet, P., Toyoda, S., Falguères, C., Hernandez, M., Tissoux, H., Moreno, D., Bahain, J-J., 2015.
567 Evaluation of ESR residual dose in quartz modern samples, an investigation on environmental
568 dependence. Quaternary Geochronology 30, 506-512.Walther, R., Zilles, D., 1994. ESR studies on
569 bleaches sedimentary quartz. Quat. Geochronol. 13 (5-7), 611–614. https://doi.org/10.1016/0277-
570 3791(94)90086-8

571

572

Residual hole concentration in recombination centres after bleaching

N. Pawlak, A. Timar-Gabor, A. Chruścińska

Supplementary Material

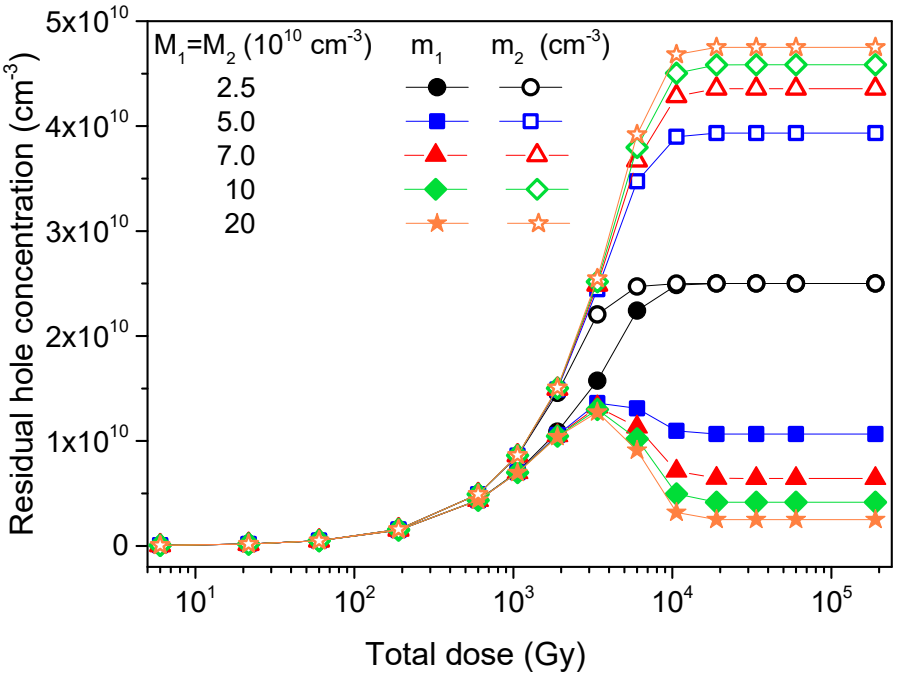

Fig. S1. The bahaviour of the dependence of RHC on the total dose which was previously absorbed of two recombination centres with clearly different recombination coefficients ($\beta_1 = 10^{-10}$ cm^{3}s^{-1}, $\beta_2 = 10^{-11}$ cm^{3}s^{-1}) for five different ratios of their concentrations M_1/M_2. M_1 is fixed and equal to 10^{11} cm^{-3}. $N_4 = 5 \times 10^{10}$ cm^{-3}.

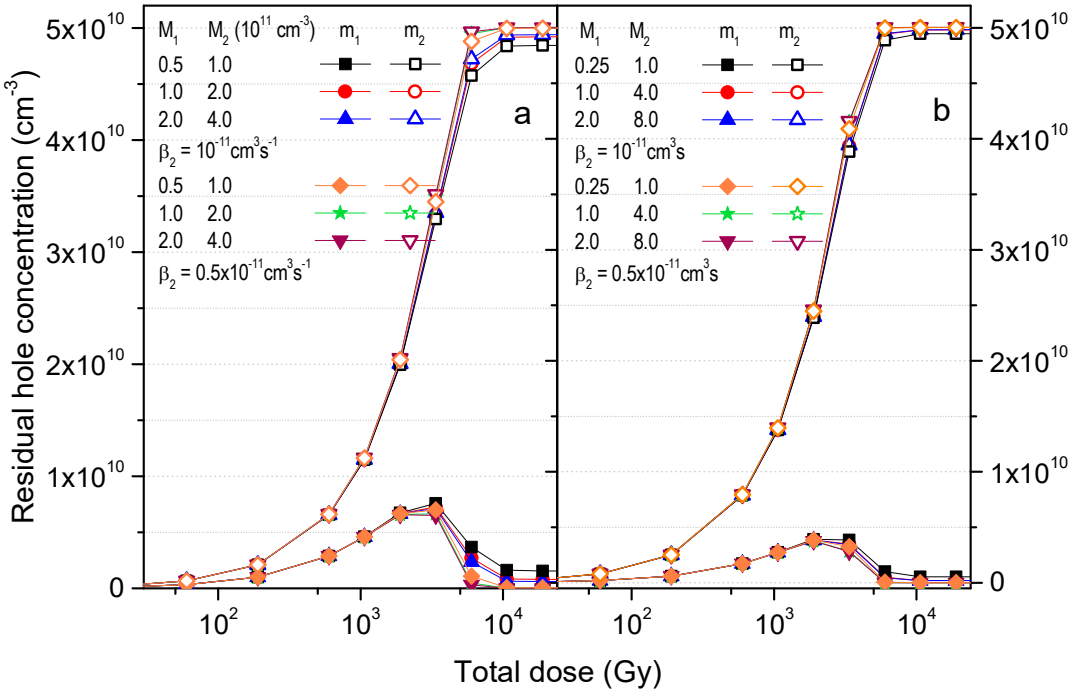

Fig. S2. Results demonstrating that the height of the peak observed in the dependence of RHC on the total dose which was previously absorbed is governed by the M_1/M_2 ratio and not by the values of individual recombination centre concentrations. The dose response curves are shown for two different relations of recombination coefficients β_1 and β_2 and for two ratios M_1/M_2: a) $M_2 = 2 \times M_1$ and b) $M_2 = 4 \times M_1$, $M_1 = 10^{11}$ cm^{-3}, $\beta_1 = 10^{-10}$ cm^{3}s^{-1}, $N_4 = 5 \times 10^{10}$ cm^{-3}.